

Design, synthesis and evaluation of novel tacrine–rhein hybrids as multifunctional agents for the treatment of Alzheimer’s disease†

Cite this: *Org. Biomol. Chem.*, 2014, **12**, 801

Su-Yi Li, Neng Jiang, Sai-Sai Xie, Kelvin D. G. Wang, Xiao-Bing Wang* and Ling-Yi Kong*

A series of tacrine–rhein hybrid compounds have been designed and synthesized as novel multifunctional potent ChE inhibitors. Most of the compounds inhibited ChEs in the nanomolar range *in vitro* effectively. Compound **10b** was one of the most potent inhibitors and was 5-fold more active than tacrine toward AChE, and it also showed a moderate BuChE inhibition with an IC₅₀ value of 200 nM. Kinetic and molecular modeling studies of **10b** also indicated that it was a mixed-type inhibitor binding simultaneously to the active and peripheral sites of AChE. In inhibition of the AChE-induced Aβ aggregation assay, compound **10b** (70.2% at 100 μM) showed the greatest inhibitory activity. In addition, **10b** showed metal-chelating property and low hepatotoxicity. These results suggested that **10b** might be an excellent multifunctional agent for AD treatment.

Received 6th October 2013,
Accepted 16th November 2013

DOI: 10.1039/c3ob42010h

www.rsc.org/obc

1. Introduction

Alzheimer’s disease (AD), the fourth leading cause of death in people over 65 years old, affects more than 24 million people worldwide.¹ Although 100 years have passed since its discovery, treating AD remains a challenge for the pharmaceutical community.² Over the past few decades, a plethora of targets have been suggested in the attempt to identify the causative factors of AD. These included deposits of aberrant proteins, namely, β-amyloid (Aβ) and τ-protein, oxidative stress, dys-homeostasis of biometals, and low levels of acetylcholine (ACh).^{3–5}

The current therapeutic options for the treatment of AD are acetylcholinesterase inhibitors (AChEIs) which are based on the cholinergic hypothesis.^{6,7} The cholinergic hypothesis of AD asserts that a decline of ACh levels leads to cognitive and memory deficits, so sustaining or recovering cholinergic function is supposed to be clinically beneficial.⁸ ACh can be degraded by two types of cholinesterases, namely acetylcholinesterase (AChE) and butyrylcholinesterase (BuChE).⁹ The crystallographic structure of AChE reveals that it has a narrow 20 Å gorge, containing two binding sites: the catalytic active site

(CAS) at the bottom and the peripheral anionic site (PAS) near the entrance of the gorge.^{10,11} Biochemical studies have indicated that AChE promotes amyloid fibril formation by interaction through the PAS of the enzyme, giving stable AChE-Aβ complexes, which are more toxic than single Aβ peptides.¹² Therefore, dual-site inhibitors that interact with both CAS and PAS appear to be a very promising therapeutic strategy, since they can simultaneously improve cognition and slow the rate of Aβ-elicited neurodegeneration.¹³ In healthy brains, AChE hydrolyzes about 80% of acetylcholine while BuChE plays a secondary role. However, as AD progresses, the activity of AChE is greatly reduced in specific brain regions while BuChE activity increases, likely as a compensation for the AChE decrease.¹⁴ Consequently, both enzymes are useful therapeutic targets for AD.

Many studies have found that overproduction of Aβ also plays an important role in the pathogenesis and development of AD, as it leads to synaptic dysfunction, formation of intra-neuronal fibrillary tangles, and eventually neuron loss.¹⁵ The deposited Aβ can cause the shrinkage of neuritis and denaturing of neurons, and it can also disrupt the calcium channels in the cell membrane, enhancing Ca²⁺ influx and leading to the disequilibrium of calcium.¹⁶ Therefore, inhibitors of the Aβ aggregation may be effective in blocking the progression of the pathology.¹⁷ Recent studies have indicated that the level of metal ions, such as iron, zinc, and copper, in the brain of AD patients is 3–7 fold higher than that of healthy individuals.¹⁸ In *in vitro* experiments the elevated concentrations of metals are able to bind to Aβ, thus promoting its aggregation.¹⁹ It has

State Key Laboratory of Natural Medicines, Department of Natural Medicinal Chemistry, China Pharmaceutical University, 24 Tong Jia Xiang, Nanjing 210009, People’s Republic of China. E-mail: cpu_lykong@126.com, xbwang@cpu.edu.cn; Tel: +86-25-83271405

† Electronic supplementary information (ESI) available. See DOI: 10.1039/c3ob42010h

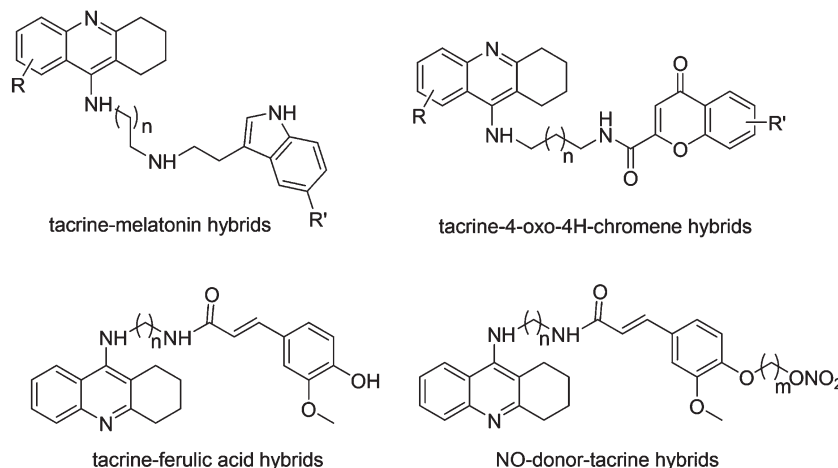


Fig. 1 Structures of some known dual-site inhibitors.

also been found that redox-active ions like Cu^{2+} and Fe^{2+} contribute to the production of reactive oxygen species and oxidative stress, which are critical for $A\beta$ neurotoxicity.^{20,21} Therefore, modulation of such biometals in the brain has been proposed as a potential therapeutic strategy for the treatment of AD.

Tacrine, the first drug approved for the treatment of AD, is a potent inhibitor of both AChE and BuChE that suffers from therapy limiting side effects, mainly liver toxicity.²² Because of the clinical effectiveness of AChEIs in general and the high potency of tacrine in particular, this structure has been widely used for application in hybrid or multitarget compounds in order to obtain potent AChEIs with other pharmacological properties.^{23,24} For example, tacrine-melatonin hybrids and tacrine-ferulic acid hybrids have been designed as potent ChEIs with antioxidant properties,²⁵ tacrine-4-oxo-4H-chromene hybrids have been designed as multifunctional agents capable of inhibiting ChE and β -secretase²⁶ and NO-donor-tacrine hybrids showed hepatoprotective properties^{9,27} (Fig. 1).

Rhein (4,5-dihydroxyanthraquinone-2-carboxylic acid) is one of the most important active components of rhubarb (*Rheum officinale*), a traditional Chinese herb to treat chronic liver disease, and shows broad-gauged pharmacological effects, such as antibacterial, anti-inflammatory and anti-tumor activities.^{28,29} Numerous reports have demonstrated that rhein has a hepatoprotective effect. Rhein can ameliorate fatty liver disease, protect hepatocytes from injury and prevent the progress of hepatic fibrosis in rats, which may be associated with the role that rhein plays in antioxidation and anti-inflammation, inhibiting the expression of TGF-beta1 and suppressing the activation of hepatic stellate cells.³⁰⁻³³ Recently, it has been reported that rhein lysinate could decrease the generation of $A\beta$ in the brain tissues of AD model mice by inhibiting the inflammatory response and oxidative stress.³⁴ These results suggest that rhein might reduce the liver toxicity caused by tacrine and be beneficial for AD treatment.

Recently, our group has reported the synthesis of tacrine-flavonoid hybrids as multifunctional ChEIs against AD.³⁵ We

continued with our research on various natural products with potential application in the AD field. In this paper, rhein was selected to hybridize with tacrine to design a series of novel hybrids exhibiting multifunctional activities. We planned to use tacrine for its inhibition of cholinesterases (ChEs) through the CAS and a rhein scaffold for its metal-chelating, hepatoprotective effects, as well as for its potential interaction with the PAS due to its aromatic character. Regarding the possible structural modification on the tacrine fragment, we focused on the 6-position substitution and changes in carbocyclic ring size of the tacrine nucleus to study possible effects on ChE inhibition. Based on the structure of AChE, we considered connecting tacrine and rhein fragments by alkylene linkers of different lengths. In order to find the optimal linker efficiently, hybrids with linkers of even-numbered carbon atoms were synthesized.

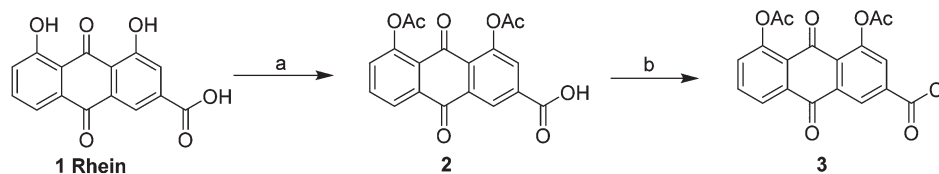
In this paper, we describe the synthesis, pharmacological evaluation, and molecular modeling of a series of novel tacrine-rhein hybrids. The pharmacological evaluation of these novel compounds include AChE and BuChE inhibition, the kinetics of enzyme inhibition, AChE-induced $A\beta$ aggregation, metal chelation, and the hepatoprotective effect. Finally, molecular modeling studies were performed to gain insight into the binding mode and structure-activity relationships of new hybrid compounds.

2. Results and discussion

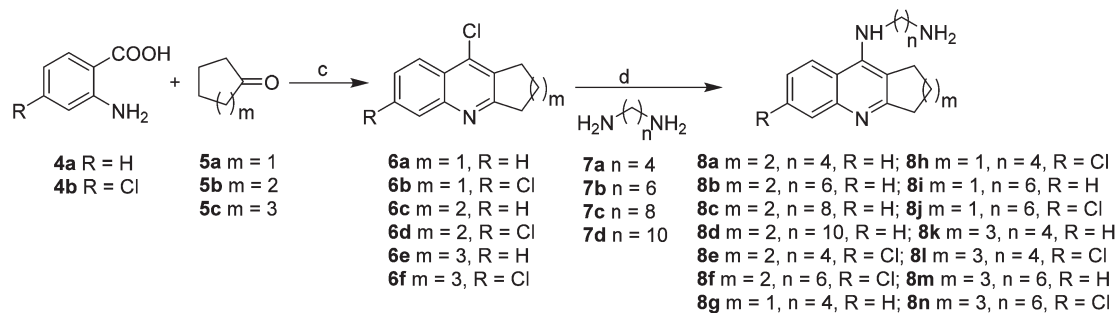
2.1. Chemistry

Total synthesis of hybrids of tacrine-rhein congeners was involved in two kinds of key intermediate compounds **3** and **8a-n**.

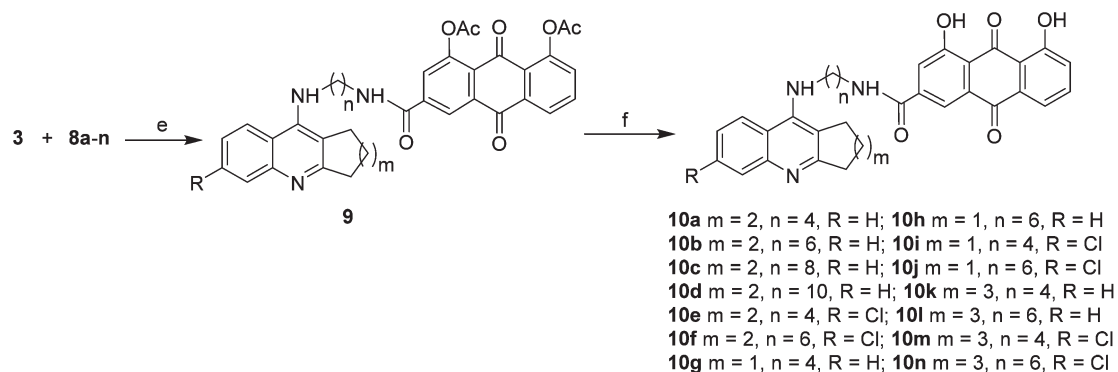
Preparation of the key intermediate compounds **8a-n** is shown in Scheme 2. The $POCl_3$ -mediated cyclodehydration reaction between **4a-b** and cycloketones **5a-c** was adapted to the corresponding chlorides **6a-f** with moderate yields (62–91%). The amination of the chlorides **8a-n** was carried out



Scheme 1 Synthesis of intermediates **2** and **3**. Reagents and conditions: (a) Ac_2O , H_2SO_4 , 3 h, reflux; (b) oxalyl chloride, DMF, CH_2Cl_2 , 1 h, 30 °C.



Scheme 2 Synthesis of intermediates **8a–n**. Reagents and conditions: (c) POCl_3 , reflux 3 h. (d) 4–5 equiv. $\text{NH}_2(\text{CH}_2)_n\text{NH}_2$, 1-pentanol, reflux 6–12 h.



Scheme 3 Synthesis of tacrine–rhein hybrids **10a–n**. Reagents and conditions: (e) Et_3N , CH_2Cl_2 , 1 h, r.t.; (f) Et_3N , acetone, H_2O , 6 h, 50 °C.

in reaction with 4 equiv. of α,ω -diamine **7a–d** in refluxing 1-pentanol for 8–16 h,³⁶ followed by removal of the solvent. The resulting mixture was diluted with dichloromethane and washed with a large amount of water. Finally the organic phase was dried with anhydrous Na_2SO_4 , concentrated *in vacuo*, and purified by column chromatography to give products **8a–n** as a pale-brown oil.

On the other hand, rhein **1** as the starting material was acetylated in the presence of Ac_2O and H_2SO_4 to afford diacerein **2**, which was chloridated with oxalyl chloride to give **3**³⁷ (Scheme 1). The obtained compound **3** was finally reacted with **8a–n** in dichloromethane to furnish desired compounds **10a–n** in moderate yields (Scheme 3).

2.2. Cholinesterase inhibitory activity

The inhibitory activity of hybrids **10a–n** and the related compound **1** against AChE (from the electric eel) and BuChE (from equine serum) was measured according to the

spectrophotometric method of Ellman *et al.*³⁸ For comparison purposes, tacrine and galanthamine were used as reference compounds. The IC_{50} values of all tested compounds and their selectivity index for AChE over BuChE are summarized in Table 1. It could be seen from Table 1 that all novel target compounds showed good inhibitory activities to both ChEs with IC_{50} values ranging from sub-micromolar to nanomolar. Among the target compounds, **10f** ($\text{IC}_{50} = 22.0$ nM) showed the most potent inhibitory activity for AChE, which was 6 and 121 times stronger than those of the reference compounds tacrine ($\text{IC}_{50} = 135$ nM) and galantamine ($\text{IC}_{50} = 2670$ nM), respectively. In contrast, **10l** exhibited the strongest inhibition to BuChE with an IC_{50} value of 11.0 nM, which was 4- and 1154-fold more potent than those of tacrine ($\text{IC}_{50} = 45.0$ nM) and galanthamine ($\text{IC}_{50} = 12\,700$ nM). From the IC_{50} values of compounds **10a–d**, it appeared that a suitable tether for the linker between the two anchoring groups, tacrine and rhein, seemed to be 6 carbons. It also showed that the variation of chain

Table 1 Inhibition of AChE and BuChE activities, selectivity index, AChE-induced A β aggregation by the synthesized compounds

Compound	<i>m</i>	<i>n</i>	R	IC ₅₀ (nM) for AChE ^a	IC ₅₀ (nM) for BuChE ^b	Selectivity index ^c	% Inhibition of A β (1–40) aggregation ^e
1				>100 000	>100 000	—	10.5 ± 0.8
10a	2	4	H	58.7 ± 4.3	286 ± 9	4.9	66.5 ± 1.2
10b	2	6	H	27.3 ± 2.9	200 ± 7	7.3	70.2 ± 0.8
10c	2	8	H	148 ± 7	360 ± 14	2.4	63.3 ± 2.4
10d	2	10	H	220 ± 12	320 ± 16	1.4	64.1 ± 1.9
10e	2	4	Cl	40.6 ± 3.7	1234 ± 45	30.4	54.7 ± 0.7
10f	2	6	Cl	22.0 ± 1.5	773 ± 28	35.1	56.5 ± 1.6
10g	1	4	H	966 ± 24	432 ± 19	0.4	46.8 ± 1.9
10h	1	6	H	543 ± 16	219 ± 16	0.4	48.1 ± 2.0
10i	1	4	Cl	453 ± 21	8816 ± 86	19.4	41.9 ± 0.8
10j	1	6	Cl	513 ± 14	769 ± 23	1.5	42.0 ± 1.7
10k	3	4	H	173 ± 16	89.5 ± 6.5	0.5	61.2 ± 2.4
10l	3	6	H	130 ± 8	11.0 ± 0.7	0.1	64.8 ± 1.8
10m	3	4	Cl	114 ± 4	1112 ± 56	5.2	58.4 ± 1.6
10n	3	6	Cl	63.8 ± 7.5	419 ± 22	6.6	55.9 ± 1.4
Tacrine				135 ± 8	45 ± 3	0.3	6.5 ± 0.8
Galantamine				2670 ± 150	12 700 ± 205	4.8	nd
Propidium				nd ^d	nd		82 ± 2

^a Inhibitor concentration (mean ± SEM of three experiments) required for 50% inactivation of AChE. ^b Inhibitor concentration (mean ± SEM of three experiments) required for 50% inactivation of BuChE. ^c Selectivity index = IC₅₀ (BuChE)/IC₅₀ (AChE). ^d Not determined. ^e Inhibition of AChE-induced A β (1–40) aggregation, the thioflavin-T fluorescence method was used, the mean ± SEM of three independent experiments and the measurements were carried out in the presence of 100 μ M compounds.

length for the inhibitors had more influence on their inhibition of AChE than BuChE. This may be due to the conformational difference between these two enzymes. By contrast, BuChE does not have a functional peripheral site, and the active site of BuChE is wider than that of AChE. Therefore, BuChE has less restriction to inhibitors with varying linker length.

Since the IC₅₀ values of **10a** (*n* = 4, IC₅₀ = 58.7 nM) and **10b** (*n* = 6, IC₅₀ = 27.3 nM) for AChE inhibition were in the nanomolar range, we selected *n* = 4 and 6 for further study. It is already known that the chlorine atom at the 6-position increases the inhibitory potency of tacrine.³⁹ A chlorine atom was introduced to the 6-position of the tacrine moiety producing **10e–f** that resulted in a slight increase in AChE inhibition, but a significant decrease in BuChE inhibition. In comparison with **10a–b**, carbocyclic-shrunk congeners **10g–h** resulted in almost 20-fold less potency at AChE and a slight decrease in BuChE inhibition, respectively. In contrast, ring-expanded **10k–l** increased the potency against BuChE activity significantly (almost 3-fold for **10k** and 20-fold for **10l**), although there was a slight decrease against AChE activity. These results disclosed that BuChE seems to be better able than AChE to accommodate steric bulk around the catalytic site.^{40,41} The presence of a chlorine atom in the ring-expanded **10k–l** and ring-shrunk **10g–h** resulted in a slight increase in AChE inhibition and a significant decrease in BuChE inhibition.

2.3. Kinetic study of ChE inhibition

To gain information on the mechanism of inhibition, the potent inhibitor **10b** was selected for kinetic studies. The type of inhibition was elucidated from the analysis of Lineweaver–Burk plots, which were reciprocal rates versus reciprocal substrate concentrations for the different inhibitor concentrations

resulting from the substrate-velocity curves for AChE. For AChE, the plot showed both increased slopes (decreased V_{\max} , from 0.40 to 0.15) and intercepts (decreased K_m , from 0.28 to 0.15) with increasing concentration of the inhibitor (Fig. 2). This pattern indicated a mixed-type inhibition and therefore revealed that compound **10b** might be able to bind to CAS as well as PAS of AChE. In contrast, a different plot for BuChE

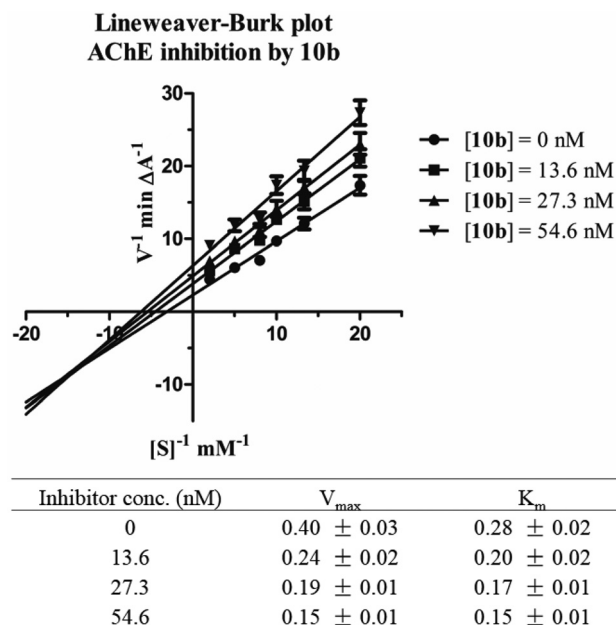


Fig. 2 Lineweaver–Burk plots resulting from the subvelocity curve of AChE activity with different substrate concentrations (0.05–0.50 mM) in the absence and presence of 13.6, 27.3, and 54.6 nM **10b**. The V_{\max} and K_m values shown in this table are the mean ± SD of three experiments.

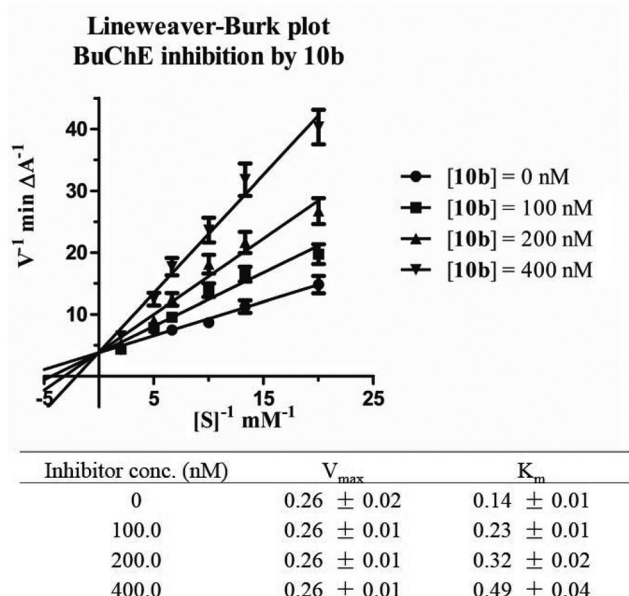


Fig. 3 Lineweaver–Burk plots resulting from the subvelocity curve of BuChE activity with different substrate concentrations (0.05–0.50 mM) in the absence and presence of 100.0, 200.0, and 400.0 nM **10b**. The V_{\max} and K_m values shown in this table are the mean \pm SD of three experiments.

was obtained, showing different K_m (from 0.14 to 0.49) and constant V_{\max} in different inhibitor concentrations (Fig. 3). This suggested a competitive inhibition, revealing that these compounds compete for the same binding site as the substrate acetylcholine.

2.4. Molecular modeling studies

To further study the interaction mode of compound **10b** for AChE, a molecular docking study was performed using the software package MOE 2008.10. The X-ray crystal structure of the TcAChE complex with bis(7)-tacrine (PDB ID 2CKM) was applied to build the starting model of AChE. As shown in Fig. 4, the tacrine moiety of **10b** was bound to the CAS of AChE, it being stacked against the phenyl ring of Phe 330 and the indole ring of Trp 84 with the ring-to-ring distance of 3.55 and 4.03 Å, respectively. The rhein moiety interacted with the indole ring of Trp 279 and Tyr70 of PAS *via* π - π stacking interactions with the distance of 3.92 and 3.72 Å, respectively. All these results clearly indicated that compound **10b** could simultaneously bind to CAS and PAS binding sites of AChE, thereby demonstrating the rationality of our molecular design.

2.5. Inhibition of AChE-induced A β (1–40) aggregation

As is known, AChE directly promotes *in vitro* the assembly of A β peptide into amyloid fibrils, forming a stable AChE–A β complex, which could cause neurotoxicity. The concomitant inhibition of the PAS of AChE, which is supposedly associated with the aggregation of A β , may turn AChEIs into potential disease modifying agents. The kinetic study of AChE inhibition and molecular modeling studies have demonstrated that the

designed compounds could interact with the PAS of AChE. To further explore the dual action of these compounds, AChE-induced A β (1–40) aggregation inhibitory activity was examined using the ThT-based fluorometric assay.^{41,42} Table 1 summarizes the anti-A β aggregation activity of the novel hybrids and reference compounds. From the results, it could be seen that all the synthesized compounds presented a good inhibitory activity on AChE-induced A β aggregation (from 41.9 to 70.2% at 100 μ M). The results indicated that **10b** (70.2% at 100 μ M) was the most potent inhibitor of AChE-induced A β aggregation, which was 11-fold more potent than tacrine and relatively weaker than the positive control propidium. From the inhibition values of compounds **10a–d**, it appeared that the linker length did not play a role in determining the inhibition of AChE-induced A β aggregation, since no significant change of the percentages of inhibition was observed along with the lengthening of the spacer length. Hybrids which consist of a unit of tacrine **10a–d** are clearly more potent than other hybrids **10g–h** and **10k–l**. The presence of a chlorine atom at position 6 of the tacrine unit leads to a slightly decreased effect.

In order to study the correlation between the AChE-induced A β aggregation inhibitory activity and AChE inhibitory potency, a scatter plot of *in vitro* inhibitory percent of AChE-induced A β aggregation *versus* IC₅₀ value for AChE inhibition was obtained and is shown in Fig. 5. Utilizing a linear fitting procedure, a statistically significant fit was obtained and it was clearly shown that the inhibitory effects for A β aggregation and AChE were positively correlated. These results appear to validate that the compound which binds both CAS and PAS of AChE simultaneously could strongly inhibit A β aggregation mediated by the enzyme.

It may be observed that the inhibitor concentration in the aggregation assay (100 μ M) is much higher than those necessary to inhibit AChE (in the sub-micromolar and nanomolar). However, as other researchers have pointed out,⁴² higher concentrations of AChE and A β are necessary, since they may speed up the process of aggregation for us to achieve the purpose of analysis. So, the inhibitor/AChE concentration values are in the same magnitude, if the concentration ratio in both Ellman's assay for the determination of the AChE inhibitory activity and the thioflavin T-based fluorometric assay for the determination of the A β antiaggregating effect is taken into account.⁴³ In this respect, it seems reasonable that similar amounts of an inhibitor can carry out simultaneously both the anticholinesterasic and the antiaggregating actions.

2.6. Metal chelating effect

To further study, the chelating effect of **10b** for metals such as Cu²⁺ and Fe²⁺ in methanol was studied by UV-vis spectrometry with wavelength ranging from 200 to 500 nm.⁴⁴ In Fig. 6a, UV-vis spectra of **10b** at increasing Cu²⁺ concentrations are shown as an example. The increase in absorbance, which could be better estimated by an inspection of the differential spectra (Fig. 6b), indicated that there was an interaction between Cu²⁺ and **10b**. A similar behavior was also observed when using Fe²⁺. These observations indicated that **10b** could effectively

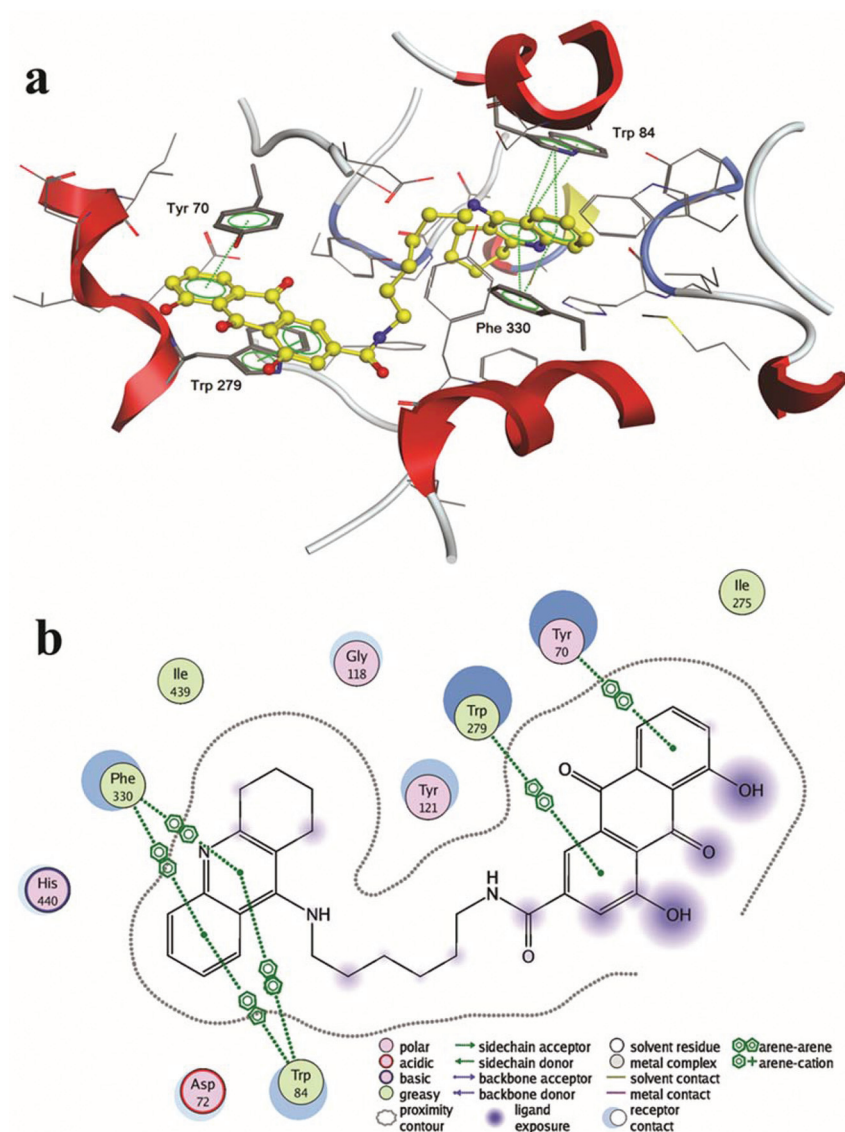


Fig. 4 (a) 3D docking model of compound **10b** with TcAChE. Atom colors: yellow-carbon atoms of **10b**, gray-carbon atoms of residues of TcAChE, dark blue-nitrogen atoms, red-oxygen atoms. The dashed lines represent the interactions between the protein and the ligand. (b) 2D schematic diagram of docking model of compound **10b** with TcAChE. The figure was prepared using the ligand interactions application in MOE.

chelate Cu^{2+} and Fe^{2+} , and thereby could serve as a metal chelator in treating AD. The ratio of the ligand/metal ion in the complex was investigated by mixing a fixed amount of the metal ion with increasing ligand; it was possible to observe that the maximum intensity of difference spectra was reached at a 1 : 1 ratio, which was taken as an indication of the stoichiometry of the complex.

In order to measure the stoichiometry of the complex **10b**- Cu^{2+} , Job's method was used⁴⁵ by preparing solutions of compound **10b** and CuCl_2 so that the sum of concentrations of both species was constant in all samples, but the proportions of both components varied between 0 and 100%. The UV absorbance differences at 250 nm were plotted vs. the mole fraction, showing a maximum at 0.53 that revealed a stoichiometry of 1 : 1 for complex **10b**- Cu^{2+} (Fig. 7).

2.7. Hepatotoxicity studies

In order to determine whether the designed tacrine-rhein hybrids had hepatotoxicity in comparison to tacrine, **10b** was selected for the assay with adult mice. After being treated with tacrine and **10b**, the heparinized serum of mice was obtained at different times, and the levels of aspartate aminotransferase (ASAT) and alanine aminotransferase (ALT) were determined (Fig. 8). In comparison to the control, tacrine caused significant hepatotoxicity, as indicated by the increased activity of ASAT and ALT. From the results, it appeared that **10b** possessed higher safety than tacrine.

For morphological studies the liver tissue was stained with hematoxylin and eosin (HE). Complete pericentral necrosis and distinct fatty degeneration of the hepatocytes of the surrounding intermediate and periportal zones were seen 30 h

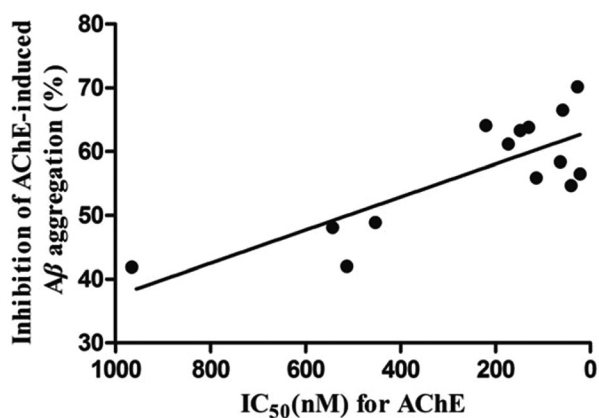


Fig. 5 Scatter plots representing *in vitro* inhibitory percent of AChE-induced A β aggregation versus IC₅₀ value for AChE inhibition for a series of tacrine–rhein hybrids.

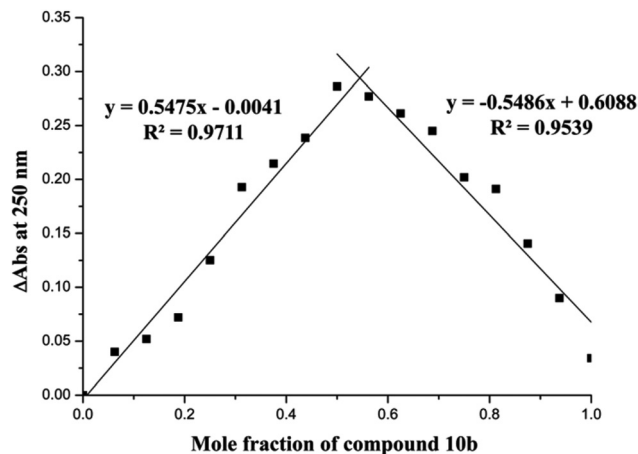


Fig. 7 Determination of the stoichiometry of complex 10b–Cu²⁺ by Job's method.

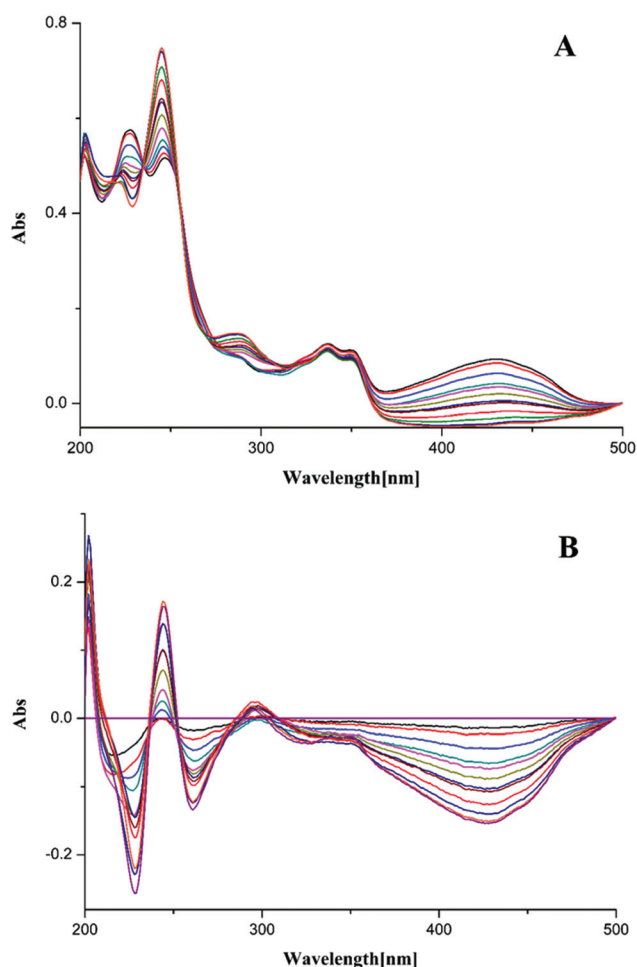


Fig. 6 (a) UV-vis (200–500 nm) absorption spectra of 10b (25 μ M) in methanol after addition of ascending amounts of CuCl₂ (2–50 μ mol L⁻¹). (b) The differential spectra due to 10b–Cu²⁺ complex formation obtained by numerical subtraction from the above spectra of those of Cu²⁺ and 10b at the corresponding concentrations.

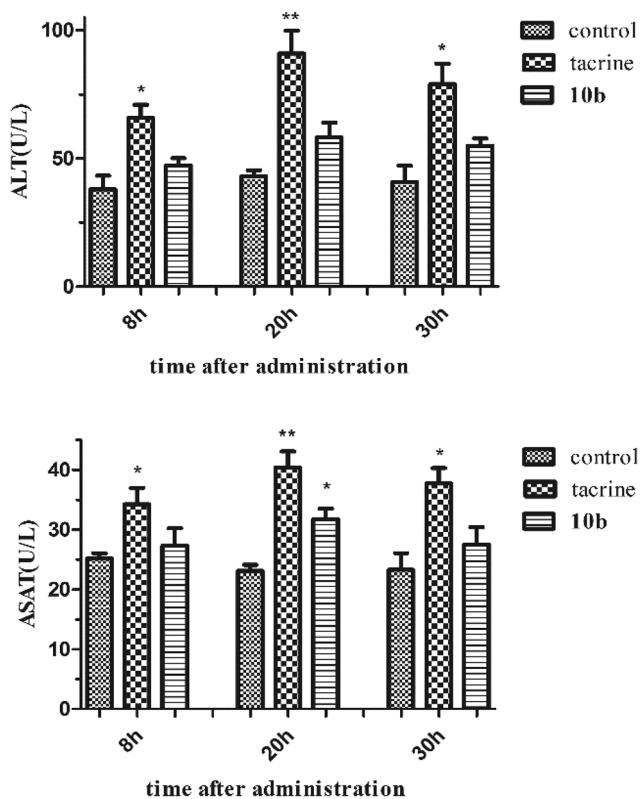


Fig. 8 ALT and ASAT activity after the administration of tacrine and 10b. Values are expressed as mean \pm SEM ($n = 8-9$; t test, compared to the control of the same time after administration, $*p \leq 0.05$, $**p \leq 0.01$).

after administration of tacrine (Fig. 9b). In contrast, only minor morphological changes were observed after the treatment with compound 10b (Fig. 9c). All these findings suggested that compound 10b could be safer than tacrine for the treatment of AD.

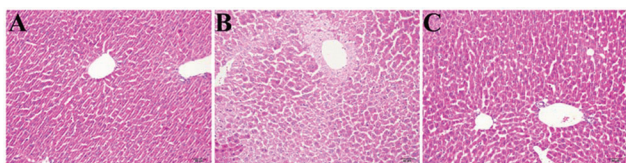


Fig. 9 Histomorphological appearance of livers of male mice after treatment with the solvent only (control) (A) or 30 h after administration of tacrine (B) or **10b** (C). HE, original magnification $\times 200$.

3. Conclusion

In conclusion, a series of tacrine–rhein hybrid compounds have been designed and synthesized as novel multifunctional potent ChE inhibitors. Most of the compounds inhibited ChEs in the nanomolar range *in vitro* effectively. Compound **10b** was one of the most potent inhibitors and was 5-fold more active than tacrine toward AChE, and it also showed a moderate BuChE inhibition with an IC_{50} value of 200 nM. Kinetic and molecular modeling studies of **10b** indicated that it was a mixed-type inhibitor binding simultaneously to active and peripheral sites of AChE. In the inhibition of the AChE-induced $A\beta$ aggregation assay, compound **10b** (70.2% at 100 μM) showed the greatest inhibitory activity. In addition, **10b** also showed metal-chelating property and low hepatotoxicity. Altogether, the multifunctional effects of the new hybrids qualified them as potential anti-AD drug candidates, and **10b** might be considered as a promising lead compound for further research.

4. Experimental section

4.1. Chemistry

All chemicals (reagent grade) used were purchased from Sinopharm Chemical Reagent Co., Ltd (China). The reaction progress was monitored using analytical thin layer chromatography (TLC) on precoated silica gel GF₂₅₄ (Qingdao Haiyang Chemical Plant, Qingdao, China) plates and the spots were detected under UV light (254 nm). The melting point was measured on an XT-4 micromelting point instrument and uncorrected. IR (KBr-disc) spectra were recorded using a Bruker Tensor 27 spectrometer. ¹H NMR and ¹³C NMR spectra were measured on a Bruker ACF-500 spectrometer at 25 °C and referenced to TMS. Chemical shifts are reported in ppm (δ) using the residual solvent line as an internal standard. The splitting patterns are designed as s, singlet; d, doublet; t, triplet; m, multiplet. The purity of all compounds was confirmed to be higher than 95% through analytical HPLC performed with an Agilent 1200 HPLC System. Mass spectra were obtained on a MS Agilent 1100 Series LC/MSD Trap mass spectrometer (ESI-MS) and a Mariner ESI-TOF spectrometer (HRESIMS), respectively. Column chromatography was performed on silica gel (90–150 μm ; Qingdao Marine Chemical Inc.).

4.1.1. General procedures for the preparation of intermediates 6a–f

9-Chloro-2,3-dihydro-1H-cyclopenta[b]quinoline (6a). General cyclization procedure: *o*-aminobenzoic acid **4a** (3 g, 22 mmol) and cyclopentanone **5a** (1.70 g, 22 mmol) were carefully added to POCl₃ (15 mL) in an ice bath. The mixture was heated under reflux for 4 h, then cooled at room temperature, and concentrated to give a slurry. The residue was diluted with EtOAc, neutralized with aqueous K₂CO₃, and washed with brine. The organic layer was dried over anhydrous Na₂CO₃ and concentrated *in vacuo* to furnish a yellow solid. The crude product was purified by silica gel chromatography with ethyl acetate and petroleum ether (1 : 10) to afford **6a** as a light yellow solid in 78.0% yield.⁴¹

6,9-Dichloro-2,3-dihydro-1H-cyclopenta[b]quinoline (6b). Compound **4b** was treated with cyclopentanone **5a** according to the general cyclization procedure to give **6b** as a pale solid in 73.2% yield.⁴⁶

9-Chloro-1,2,3,4-tetrahydroacridine (6c). Compound **4a** was treated with cyclohexanone **5b** according to the general cyclization procedure to give **6c** as a pale solid in 81.0% yield.⁴¹

6,9-Dichloro-1,2,3,4-tetrahydroacridine (6d). Compound **4b** was treated with cyclohexanone **5b** according to the general cyclization procedure to give **6d** as a pale solid in 91.0% yield.⁴⁷

11-Chloro-7,8,9,10-tetrahydro-6H-cyclohepta[b]quinoline (6e). Compound **4a** was treated with cycloheptanone **5c** according to the general cyclization procedure to give **6e** as a pale solid in 62.0% yield.⁴¹

3,11-Dichloro-7,8,9,10-tetrahydro-6H-cyclohepta[b]quinoline (6f). Compound **4b** was treated with cycloheptanone **5c** according to the general cyclization procedure to give **6f** as a pale solid in 62.0% yield.⁴⁸

4.1.2. General procedures for the preparation of intermediates 8a–n

N¹-(1,2,3,4-Tetrahydroacridin-9-yl)butane-1,4-diamine (8a). Intermediate **6c** (2.0 g, 9.3 mmol), butanediamine **7a** (3.0 g, 37.1 mmol), catalytic amount of KI (0.02 g) and 1-pentanol (4 mL) were combined and heated to reflux (160 °C) for 12 h. After cooling to room temperature, the mixture was diluted with CH₂Cl₂ (30 mL) and then washed with 10% NaOH (30 mL \times 3) and water (30 mL \times 3). The organic layer was dried over anhydrous K₂CO₃, filtered, concentrated *in vacuo*, and purified by silica gel chromatography with CH₂Cl₂–MeOH–Et₃N (100 : 20 : 0.5) as an eluent to afford compound **8a** as a yellow oil in 52.0% yield.⁹

N¹-(1,2,3,4-Tetrahydroacridin-9-yl)hexane-1,6-diamine (8b). Intermediate **6c** was treated with hexanediamine **7b** according to the general procedure like **8a** to give the desired product **8b** as a yellow oil in 57.6% yield.⁹

N¹-(1,2,3,4-Tetrahydroacridin-9-yl)octane-1,8-diamine (8c). Intermediate **6c** was treated with diaminoctane **7c** according to the general procedure to give the desired product **8c** as a yellow oil in 42.3% yield.⁹

N¹-(1,2,3,4-Tetrahydroacridin-9-yl)decane-1,10-diamine (8d). Intermediate **6c** was treated with diaminodecane **7d** according

to the general procedure to give the desired product **8d** as a yellow oil in 54.5% yield.⁴⁷

*N*¹-(6-Chloro-1,2,3,4-tetrahydroacridin-9-yl)butane-1,4-diamine (**8e**). Intermediate **6d** was treated with butanediamine **7a** according to the general procedure to give the desired product **8e** as a yellow oil in 48.5% yield.⁴⁷

*N*¹-(6-Chloro-1,2,3,4-tetrahydroacridin-9-yl)hexane-1,6-diamine (**8f**). Intermediate **6d** was treated with hexanediamine **7b** according to the general procedure to give the desired product **8f** as a yellow oil in 55.2% yield.⁴⁷

*N*¹-(2,3-Dihydro-1H-cyclopenta[b]quinolin-9-yl)butane-1,4-diamine (**8g**). Intermediate **6a** was treated with butanediamine **7a** according to the general procedure to give the desired product **8g** as a yellow oil in 53.0% yield.⁴¹

*N*¹-(6-Chloro-2,3-dihydro-1H-cyclopenta[b]quinolin-9-yl)butane-1,4-diamine (**8h**). Intermediate **6b** was treated with butanediamine **7a** according to the general procedure to give the desired product **8h** as a yellow oil in 62.4% yield; ¹H NMR (500 MHz, CD₃OD) δ 8.03 (d, *J* = 9.1 Hz, 1H), 7.68 (d, *J* = 2.2 Hz, 1H), 7.30 (dd, *J* = 9.0, 2.2 Hz, 1H), 3.62 (t, *J* = 7.1 Hz, 2H), 3.23 (t, *J* = 7.2 Hz, 2H), 2.94 (t, *J* = 7.8 Hz, 2H), 2.67 (t, *J* = 7.1 Hz, 2H), 2.12 (p, *J* = 7.6 Hz, 2H), 1.71–1.64 (m, 2H), 1.61–1.52 (m, 2H); ESI-MS *m/z*: 290.1 [M + H]⁺.

*N*¹-(2,3-Dihydro-1H-cyclopenta[b]quinolin-9-yl)hexane-1,6-diamine (**8i**). Intermediate **6a** was treated with hexanediamine **7b** according to the general procedure to give the desired product **8i** as a yellow oil in 64.2% yield.⁴⁹

*N*¹-(6-Chloro-2,3-dihydro-1H-cyclopenta[b]quinolin-9-yl)hexane-1,6-diamine (**8j**). Intermediate **6b** was treated with hexanediamine **7b** according to the general procedure to give the desired product **8j** as a yellow oil, in 48.5% yield; ¹H NMR (500 MHz, CD₃OD) δ 8.04 (d, *J* = 9.1 Hz, 1H), 7.69 (d, *J* = 2.2 Hz, 1H), 7.31 (dd, *J* = 9.1, 2.2 Hz, 1H), 3.61 (t, *J* = 7.2 Hz, 2H), 3.23 (t, *J* = 7.2 Hz, 2H), 2.95 (t, *J* = 7.8 Hz, 2H), 2.66–2.58 (m, 2H), 2.13 (p, *J* = 7.5 Hz, 2H), 1.66 (h, *J* = 6.7, 6.2 Hz, 2H), 1.51–1.44 (m, 2H), 1.45–1.33 (m, 4H); ESI-MS *m/z*: 318.2 [M + H]⁺.

*N*¹-(7,8,9,10-Tetrahydro-6H-cyclohepta[b]quinolin-11-yl)butane-1,4-diamine (**8k**). Intermediate **6e** was treated with butanediamine **7a** according to the general procedure to give the desired product **8k** as a yellow oil in 60.4% yield.⁴¹

*N*¹-(3-Chloro-7,8,9,10-tetrahydro-6H-cyclohepta[b]quinolin-11-yl)butane-1,4-diamine (**8l**). Intermediate **6f** was treated with butanediamine **7a** according to the general procedure to give the desired product **8l** as a yellow oil in 68.5% yield; ¹H NMR (500 MHz, CD₃OD) δ 8.14 (d, *J* = 8.8, 1H), 7.86 (d, *J* = 2.1 Hz, 1H), 7.49 (dd, *J* = 8.8, 2.1 Hz, 1H), 3.40–3.36 (m, 2H), 3.20–3.12 (m, 2H), 3.07–2.96 (m, 2H), 2.74–2.63 (m, 2H), 1.98–1.95 (m, 2H), 1.85–1.78 (m, 4H), 1.75–1.66 (m, 2H), 1.61–1.52 (m, 2H); ESI-MS *m/z*: 318.2 [M + H]⁺.

*N*¹-(7,8,9,10-Tetrahydro-6H-cyclohepta[b]quinolin-11-yl)hexane-1,6-diamine (**8m**). Intermediate **6e** was treated with hexanediamine **7b** according to the general procedure to give the desired product **8m** as a yellow oil in 57.6% yield; ¹H NMR (500 MHz, CD₃OD) δ 8.09 (d, *J* = 8.5, 1.3 Hz, 1H), 7.83 (dd, *J* = 8.4, 1.2 Hz, 1H), 7.58 (ddd, *J* = 8.3, 6.9, 1.4 Hz, 1H), 7.43 (ddd, *J* = 8.3, 6.8, 1.3 Hz, 1H), 3.36–3.32 (m, 2H), 3.16–3.09 (m, 2H), 3.03–2.94

(m, 2H), 2.66–2.57 (m, 2H), 1.92 (dq, *J* = 11.8, 5.8 Hz, 2H), 1.76 (dp, *J* = 16.5, 5.8 Hz, 4H), 1.64 (p, *J* = 7.8, 7.3 Hz, 2H), 1.50–1.42 (m, 2H), 1.40–1.30 (m, 4H); ESI-MS *m/z*: 312.2 [M + H]⁺.

*N*¹-(3-Chloro-7,8,9,10-tetrahydro-6H-cyclohepta[b]quinolin-11-yl)hexane-1,6-diamine (**8n**). Intermediate **6f** was treated with hexanediamine **7b** according to the general procedure to give the desired product **8n** as a yellow oil in 57.6% yield; ¹H NMR (500 MHz, CD₃OD) δ 8.08 (d, *J* = 9.0 Hz, 1H), 7.80 (d, *J* = 2.2 Hz, 1H), 7.39 (dd, *J* = 9.0, 2.2 Hz, 1H), 3.37–3.32 (m, 2H), 3.15–3.07 (m, 2H), 3.00–2.92 (m, 2H), 2.63–2.54 (m, 2H), 1.93–1.89 (m, 2H), 1.79–1.71 (m, 4H), 1.68–1.60 (m, 2H), 1.44 (p, *J* = 7.3 Hz, 2H), 1.39–1.28 (m, 4H); ESI-MS *m/z*: 346.2 [M + H]⁺.

4.1.3. General procedures for the preparation of compounds 10a–n. General procedure: to anhydrous dichloromethane (25 mL) were added oxalyl chloride (0.42 mL, 4.83 mmol) and DMF (0.25 mL). The solution was stirred for 0.5 h at room temperature and diacerein **2** (1 g, 2.65 mmol) was added. The mixture was heated to 30 °C for 1 h. All solvents were removed under reduced pressure to get acyl chloride **3**, which was dissolved in dichloromethane (60 mL). This solution was added to **8** (2.65 mmol) and triethylamine (0.65 mL, 4.62 mmol) in dichloromethane (10 mL) by dripping at room temperature. When the reaction was complete, it was diluted with dichloromethane, washed with water, followed by brine solution. The organic layer was dried over anhydrous Na₂SO₄ and concentrated under reduced pressure. The crude product **9** was dissolved in acetone (30 mL) without purification. Triethylamine (3 mL, 21.35 mmol) and water (2 mL) were added. The solution was heated to 50 °C for 6 h, the solvent was removed under reduced pressure and the residue was poured into water, and the pH was adjusted to 6 with 10% HCl. The water layer was extracted using dichloromethane and the organic layer was separated, washed with brine, dried over Na₂SO₄, and concentrated under reduced pressure to give the crude product, which was purified by chromatography (CH₂Cl₂–MeOH = 10 : 1) on silica gel to afford **10** as a solid.

4,5-Dihydroxy-9,10-dioxo-N-(4-((1,2,3,4-tetrahydroacridin-9-yl)amino)butyl)-9,10-dihydroanthracene-2-carboxamide (**10a**). Intermediate **9** was treated with **8a** according to the general procedure to give the desired product **10a** as a red solid in 59.5% yield, m.p. 168–170 °C; IR (KBr) ν 3450.3, 2923.7, 1635.3, 1562.7, 1453.4, 1401.5, 1271.1, 1197.5, 1080.2, cm⁻¹; ¹H NMR (500 MHz, CDCl₃) δ 8.02 (d, *J* = 1.7 Hz, 1H), 7.96–7.91 (m, 1H), 7.88 (dd, *J* = 8.3, 1.3 Hz, 1H), 7.83 (dd, *J* = 7.6, 1.1 Hz, 1H), 7.76–7.68 (m, 2H), 7.52 (ddd, *J* = 8.2, 6.7, 1.4 Hz, 1H), 7.33 (td, *J* = 8.3, 1.3 Hz, 2H), 6.68 (s, 1H), 3.56–3.52 (m, 4H), 3.08–2.99 (m, 2H), 2.72 (q, *J* = 6.0, 4.2 Hz, 2H), 1.92–1.89 (m, 4H), 1.82–1.75 (m, 4H). ¹³C NMR (125 MHz, CDCl₃) δ 192.60, 181.11, 165.07, 162.86, 162.76, 150.60, 142.40, 137.63, 134.00, 133.45, 128.51, 125.06, 123.96, 123.42, 122.61, 120.37, 120.23, 118.97, 117.39, 117.07, 115.82, 48.86, 40.07, 29.71, 29.07, 27.16, 24.90, 23.03, 22.70; ESI-MS *m/z*: 536.2 [M + H]⁺; HRMS: calcd for C₃₂H₃₀N₃O₅ [M + H]⁺, 536.2180, found 536.2179.

4,5-Dihydroxy-9,10-dioxo-N-(6-((1,2,3,4-tetrahydroacridin-9-yl)amino)hexyl)-9,10-dihydroanthracene-2-carboxamide (**10b**). Intermediate **9**

was treated with **8b** according to the general procedure to give the desired product **10b** as a dark yellow solid in 65.0% yield, m.p. 183–185 °C; IR (KBr) ν 3450.3, 2933.8, 1625.7, 1546.1, 1474.3, 1384.6, 1272.4, 1210.0, 1162.7, 1084.2 cm^{-1} ; ^1H NMR (500 MHz, CDCl_3) δ 8.01 (s, 1H), 7.91 (dd, $J = 15.9, 8.5$ Hz, 2H), 7.82 (d, $J = 7.5$ Hz, 1H), 7.78–7.65 (m, 2H), 7.52 (t, $J = 7.7$ Hz, 1H), 7.32 (dd, $J = 8.5, 5.4$ Hz, 2H), 6.59–6.48 (m, 1H), 4.08 (s, 1H), 3.52–3.47 (m, 4H), 3.07–3.05 (m, 2H), 2.70–2.68 (m, 2H), 1.93–1.90 (m, 4H), 1.72–1.64 (m, 4H), 1.51–1.41 (m, 4H). ^{13}C NMR (125 MHz, CDCl_3) δ 192.73, 181.26, 165.17, 162.99, 162.88, 154.13, 142.78, 137.76, 134.10, 133.59, 125.16, 124.22, 124.10, 123.57, 123.18, 120.49, 118.48, 117.43, 117.30, 115.97, 100.14, 49.17, 40.26, 31.58, 29.86, 29.55, 26.69, 26.57, 24.69, 22.97, 22.46; ESI-MS m/z : 562.2 $[\text{M} - \text{H}]^-$; HRMS: calcd for $\text{C}_{34}\text{H}_{32}\text{N}_3\text{O}_5$ $[\text{M} - \text{H}]^-$, 562.2347, found 562.2349.

4,5-Dihydroxy-9,10-dioxo-N-(8-((1,2,3,4-tetrahydroacridin-9-yl)amino)octyl)-9,10-dihydroanthracene-2-carboxamide (**10c**). Intermediate **9** was treated with **8c** according to the general procedure to give the desired product **10c** as a red solid in 56.2% yield, m.p. 132–133 °C; IR (KBr) ν 3445.8, 2925.6, 1634.2, 1474.7, 1399.8, 1272.1, 1201.1, 1080.5 cm^{-1} ; ^1H NMR (500 MHz, CDCl_3) δ 8.01 (d, $J = 1.7$ Hz, 1H), 7.90 (dd, $J = 17.1, 8.5$ Hz, 2H), 7.78 (d, $J = 7.4$ Hz, 1H), 7.73–7.65 (m, 2H), 7.51 (t, $J = 7.5$ Hz, 1H), 7.38–7.22 (m, 2H), 6.83–6.68 (m, 1H), 4.11 (s, 1H), 3.51–3.44 (m, 4H), 3.06–3.04 (m, 2H), 2.68–2.63 (m, 2H), 1.90 (p, $J = 3.3$ Hz, 4H), 1.69–1.60 (m, 4H), 1.44–1.28 (m, 8H). ^{13}C NMR (125 MHz, CDCl_3) δ 192.65, 181.20, 165.14, 162.91, 162.83, 151.50, 142.92, 137.69, 134.01, 133.54, 128.93, 127.88, 125.10, 123.93, 123.54, 123.10, 120.42, 119.75, 117.36, 115.91, 115.33, 100.12, 49.44, 40.47, 33.43, 31.76, 29.84, 29.52, 29.18, 26.84, 24.78, 23.07, 22.68; ESI-MS m/z : 590.3 $[\text{M} - \text{H}]^-$; HRMS: calcd for $\text{C}_{36}\text{H}_{36}\text{N}_3\text{O}_5$ $[\text{M} - \text{H}]^-$, 590.2674, found 590.2677.

4,5-Dihydroxy-9,10-dioxo-N-(10-((1,2,3,4-tetrahydroacridin-9-yl)amino)decyl)-9,10-dihydroanthracene-2-carboxamide (**10d**). Intermediate **9** was treated with **8d** according to the general procedure to give the desired product **10d** as a dark yellow solid in 68.5% yield, m.p. 141–143 °C; IR (KBr) ν 3455.2, 2924.1, 1626.2, 1541.5, 1473.3, 1401.1, 1272.1, 1205.4, 1162.6, 1082.0 cm^{-1} ; ^1H NMR (500 MHz, CDCl_3) δ 8.04 (d, $J = 1.7$ Hz, 1H), 7.96–7.91 (m, 1H), 7.89 (d, $J = 8.5$ Hz, 1H), 7.81 (dd, $J = 7.4, 1.2$ Hz, 1H), 7.73 (d, $J = 1.7$ Hz, 1H), 7.68 (t, $J = 7.9$ Hz, 1H), 7.57–7.48 (m, 1H), 7.37–7.27 (m, 2H), 6.69–6.59 (m, 1H), 4.01 (s, 1H), 3.54–3.41 (m, 4H), 3.04 (t, $J = 5.8$ Hz, 2H), 2.73–2.64 (m, 2H), 1.95–1.82 (m, 4H), 1.68–1.60 (m, 4H), 1.41–1.35 (m, 4H), 1.34–1.23 (m, 8H). ^{13}C NMR (125 MHz, CDCl_3) δ 192.74, 181.29, 165.07, 162.94, 162.89, 142.92, 137.71, 134.09, 133.59, 128.68, 125.13, 123.82, 123.57, 123.04, 120.46, 117.41, 117.33, 115.95, 49.58, 40.57, 33.83, 31.87, 29.61, 29.46, 29.39, 29.35, 29.27, 27.02, 26.97, 24.88, 23.17, 22.84; ESI-MS m/z : 618.3 $[\text{M} - \text{H}]^-$; HRMS: calcd for $\text{C}_{38}\text{H}_{40}\text{N}_3\text{O}_5$ $[\text{M} - \text{H}]^-$, 618.2987, found 618.2984.

N-(4-((6-Chloro-1,2,3,4-tetrahydroacridin-9-yl)amino)butyl)-4,5-dihydroxy-9,10-dioxo-9,10-dihydroanthracene-2-carboxamide (**10e**). Intermediate **9** was treated with **8e** according to the

general procedure to give the desired product **10e** as a red solid in 69.4% yield, m.p. 115–117 °C; IR (KBr) ν 3457.0, 2935.6, 1629.2, 1554.6, 1477.3, 1450.4, 1401.1, 1269.6, 1200.7, 1157.2, 1082.3 cm^{-1} ; ^1H NMR (500 MHz, CDCl_3) δ 7.98 (d, $J = 1.7$ Hz, 1H), 7.83 (d, $J = 9.0$ Hz, 1H), 7.81–7.77 (m, 2H), 7.72–7.65 (m, 2H), 7.31 (dd, $J = 8.3, 1.1$ Hz, 1H), 7.22 (dd, $J = 9.0, 2.2$ Hz, 1H), 6.78 (t, $J = 5.9$ Hz, 1H), 5.30 (s, 1H), 4.03 (s, 1H), 3.56–3.43 (m, 4H), 3.03–2.94 (m, 2H), 2.70–2.62 (m, 2H), 1.92–1.87 (m, 4H), 1.80–1.73 (m, 4H). ^{13}C NMR (125 MHz, CDCl_3) δ 192.61, 181.11, 165.30, 162.93, 162.78, 159.66, 150.66, 142.47, 137.74, 134.28, 134.01, 133.48, 130.12, 127.53, 125.16, 124.64, 124.45, 123.46, 120.45, 118.60, 117.42, 117.23, 116.43, 115.86, 49.07, 40.15, 34.01, 29.19, 27.20, 24.85, 23.03, 22.71; ESI-MS m/z : 570.2 $[\text{M} + \text{H}]^+$; HRMS: calcd for $\text{C}_{32}\text{H}_{29}\text{ClN}_3\text{O}_5$ $[\text{M} + \text{H}]^+$, 570.1790, found 570.1786.

N-(6-((6-Chloro-1,2,3,4-tetrahydroacridin-9-yl)amino)hexyl)-4,5-dihydroxy-9,10-dioxo-9,10-dihydroanthracene-2-carboxamide (**10f**). Intermediate **9** was treated with **8f** according to the general procedure to give the desired product **10f** as a red solid in 58.0% yield, m.p. 153–154 °C; IR (KBr) ν 3448.5, 2931.6, 1629.3, 1510.1, 1475.5, 1401.3, 1271.3, 1199.5, 1160.0, 1086.2 cm^{-1} ; ^1H NMR (500 MHz, $\text{DMSO}-d_6$) δ 8.84 (t, $J = 5.5$ Hz, 1H), 8.18–8.08 (m, 2H), 7.84 (t, $J = 7.9$ Hz, 1H), 7.78–7.72 (m, 2H), 7.65 (d, $J = 2.3$ Hz, 1H), 7.42 (d, $J = 8.3$ Hz, 1H), 7.31 (dd, $J = 9.0, 2.3$ Hz, 1H), 3.44–3.39 (m, 4H), 2.86 (t, $J = 6.1$ Hz, 2H), 2.67 (t, $J = 5.9$ Hz, 2H), 1.82–1.76 (m, 4H), 1.61–1.65 (m, 2H), 1.65–1.60 (m, 2H), 1.36–1.30 (m, 4H). ^{13}C NMR (125 MHz, $\text{DMSO}-d_6$) δ 192.71, 181.25, 165.07, 162.99, 162.86, 154.18, 142.84, 137.79, 134.15, 133.61, 125.19, 124.28, 124.17, 123.51, 123.13, 120.36, 118.45, 117.39, 117.28, 115.95, 100.10, 49.19, 40.29, 31.66, 29.94, 29.57, 26.76, 26.65, 24.69, 22.98, 22.47; ESI-MS m/z : 598.2 $[\text{M} + \text{H}]^+$; HRMS: calcd for $\text{C}_{34}\text{H}_{33}\text{ClN}_3\text{O}_5$ $[\text{M} + \text{H}]^+$, 598.2103, found 598.2101.

N-(4-((2,3-Dihydro-1H-cyclopenta[b]quinolin-9-yl)amino)butyl)-4,5-dihydroxy-9,10-dioxo-9,10-dihydroanthracene-2-carboxamide (**10g**). Intermediate **9** was treated with **8g** according to the general procedure to give the desired product **10g** as a red solid in 59.5% yield, m.p. 228–230 °C; IR (KBr) ν 3452.6, 2956.3, 1642.9, 1588.2, 1571.1, 1535.8, 1400.2, 1301.9, 1291.9, 1266.5, 1201.2 cm^{-1} ; ^1H NMR (500 MHz, $\text{DMSO}-d_6$) δ 8.88 (brs, 1H), 8.23 (d, $J = 8.5$ Hz, 1H), 8.10 (brs, 1H), 7.78–7.68 (m, 2H), 7.68–7.66 (m, 1H), 7.57–7.54 (m, 1H), 7.39–7.36 (m, 2H), 6.99 (s, 1H), 3.59 (q, $J = 6.5$ Hz, 2H), 3.19 (t, $J = 7.3$ Hz, 4H), 2.89 (t, $J = 7.8$ Hz, 2H), 2.02 (p, $J = 7.6$ Hz, 2H), 1.69–1.64 (m, 4H). ^{13}C NMR (125 MHz, $\text{DMSO}-d_6$) δ 191.43, 180.24, 169.44, 169.31, 164.68, 150.70, 150.37, 147.02, 140.14, 134.96, 134.61, 134.47, 133.36, 130.74, 129.51, 127.35, 125.68, 124.84, 122.63, 121.95, 117.32, 114.43, 45.23, 40.14, 34.83, 29.90, 27.46, 23.23, 21.48; ESI-MS m/z : 556.2 $[\text{M} - \text{H}]^-$; HRMS: calcd for $\text{C}_{31}\text{H}_{26}\text{N}_3\text{O}_5$ $[\text{M} - \text{H}]^-$, 556.1878, found 556.1877.

N-(6-((2,3-Dihydro-1H-cyclopenta[b]quinolin-9-yl)amino)hexyl)-4,5-dihydroxy-9,10-dioxo-9,10-dihydroanthracene-2-carboxamide (**10h**). Intermediate **9** was treated with **8i** according to the general procedure to give the desired product **10h** as a red solid in 64.3% yield, m.p. 116–118 °C; IR (KBr) ν 3453.7, 2925.0, 1631.9, 1474.6, 1400.7, 1271.6, 1201.1, 1157.9,

1082.9 cm⁻¹; ¹H NMR (500 MHz, DMSO-*d*₆) δ 8.84 (t, *J* = 5.6 Hz, 1H), 8.17 (dd, *J* = 8.5, 1.4 Hz, 1H), 8.09 (d, *J* = 1.7 Hz, 1H), 7.80 (t, *J* = 7.9 Hz, 1H), 7.74–7.69 (m, 2H), 7.66–7.32 (m, 1H), 7.51–7.48 (m, 1H), 7.38 (d, *J* = 8.4 Hz, 1H), 7.34–7.30 (m, 1H), 6.64 (t, *J* = 6.1 Hz, 1H), 3.51 (q, *J* = 6.7 Hz, 2H), 3.29 (q, *J* = 6.6 Hz, 2H), 3.15 (t, *J* = 7.2 Hz, 2H), 2.85 (t, *J* = 7.8 Hz, 2H), 2.01 (p, *J* = 7.6 Hz, 2H), 1.62–1.53 (m, 4H), 1.42–1.33 (m, 4H). ¹³C NMR (125 MHz, DMSO-*d*₆) δ 191.19, 181.08, 171.83, 167.13, 163.85, 161.50, 161.42, 147.04, 146.74, 141.79, 137.32, 133.50, 133.28, 128.01, 127.45, 124.49, 123.13, 122.48, 121.61, 119.21, 118.60, 117.30, 117.27, 116.05, 111.82, 44.02, 33.87, 30.61, 30.56, 28.71, 26.15, 25.78, 22.62, 20.95; ESI-MS *m/z*: 548.2 [M – H]⁻; HRMS: calcd for C₃₃H₃₀N₃O₅ [M – H]⁻, 548.2191, found 548.2192.

N-(4-((6-Chloro-2,3-dihydro-1H-cyclopenta[b]quinolin-9-yl)amino)butyl)-4,5-dihydroxy-9,10-dioxo-9,10-dihydroanthracene-2-carboxamide (**10i**). Intermediate **9** was treated with **8h** according to the general procedure to give the desired product **10i** as a yellow solid in 55.0% yield, m.p. 153–155 °C; IR (KBr) ν 3456.3, 2951.8, 1783.0, 1763.7, 1677.2, 1637.5, 1566.9, 1400.7, 1366.5, 1193.6, 1022.3 cm⁻¹; ¹H NMR (500 MHz, CDCl₃) δ 8.39 (d, *J* = 1.9 Hz, 1H), 8.16 (dd, *J* = 7.9, 1.3 Hz, 1H), 7.89 (d, *J* = 1.8 Hz, 1H), 7.81–7.75 (m, 2H), 7.74–7.70 (m, 1H), 7.41 (dd, *J* = 8.0, 1.3 Hz, 1H), 7.23 (dd, *J* = 9.1, 2.2 Hz, 1H), 7.09–6.99 (m, 1H), 5.05 (s, 1H), 3.61 (q, *J* = 6.1, 5.6 Hz, 2H), 3.53 (q, *J* = 6.3 Hz, 2H), 3.13 (t, *J* = 7.3 Hz, 2H), 2.98 (t, *J* = 7.8 Hz, 2H), 2.10 (p, *J* = 7.6 Hz, 3H), 1.81–1.70 (m, 4H). ¹³C NMR (125 MHz, CDCl₃) δ 191.47, 180.28, 169.49, 169.36, 164.72, 150.75, 150.40, 147.04, 140.19, 135.02, 134.65, 134.52, 134.40, 130.77, 129.57, 127.41, 125.71, 124.88, 122.65, 121.96, 117.37, 114.46, 45.28, 40.04, 34.76, 29.85, 27.02, 23.18, 21.18; ESI-MS *m/z*: 556.2 [M + H]⁺; HRMS: calcd for C₃₁H₂₇ClN₃O₅ [M + H]⁺, 556.1634, found 556.1633.

N-(6-((3-Chloro-2,3-dihydro-1H-cyclopenta[b]quinolin-9-yl)amino)hexyl)-4,5-dihydroxy-9,10-dioxo-9,10-dihydroanthracene-2-carboxamide (**10j**). Intermediate **9** was treated with **8j** according to the general procedure to give the desired product **10j** as a red solid in 53.6% yield, m.p. 118–120 °C; IR (KBr) ν 3452.3, 2924.1, 1635.7, 1499.6, 1483.5, 1400.7, 1286.8, 1198.3, 1080.4 cm⁻¹; ¹H NMR (500 MHz, DMSO-*d*₆) δ 8.85 (t, *J* = 5.6 Hz, 1H), 8.18 (d, *J* = 9.0 Hz, 1H), 8.10 (d, *J* = 1.7 Hz, 1H), 7.82 (t, *J* = 7.9 Hz, 1H), 7.75–7.72 (m, 2H), 7.60 (d, *J* = 2.3 Hz, 1H), 7.40 (d, *J* = 8.4 Hz, 1H), 7.30 (dd, *J* = 9.0, 2.4 Hz, 1H), 6.69–6.59 (m, 1H), 3.49 (q, *J* = 6.8 Hz, 2H), 3.29 (q, *J* = 6.6 Hz, 3H), 3.14 (t, *J* = 7.2 Hz, 2H), 2.82 (t, *J* = 7.8 Hz, 2H), 1.99 (p, *J* = 8.8, 8.2 Hz, 2H), 1.63–1.50 (m, 4H), 1.41–1.34 (m, 4H). ¹³C NMR (125 MHz, DMSO-*d*₆) δ 191.43, 181.05, 163.81, 161.35, 161.12, 141.88, 137.46, 134.23, 133.50, 133.31, 132.46, 126.35, 124.44, 123.88, 123.15, 122.28, 119.35, 117.47, 116.07, 112.28, 43.98, 34.05, 30.54, 28.64, 26.10, 25.75, 22.52, 20.72; ESI-MS *m/z*: 584.2 [M + H]⁺; HRMS: calcd for C₃₃H₃₁ClN₃O₅ [M + H]⁺, 584.1947, found 584.1945.

N-(4-((3-Chloro-7,8,9,10-tetrahydro-6H-cyclohepta[b]quinolin-11-yl)amino)butyl)-4,5-dihydroxy-9,10-dioxo-9,10-dihydroanthracene-2-carboxamide (**10k**). Intermediate **9** was treated with **8k** according to the general procedure to give the desired product

10k as a red solid in 57.5% yield, m.p. 209–211 °C; IR (KBr) ν 3449.8, 2924.5, 1631.8, 1558.7, 1479.5, 1452.7, 1400.9, 1270.8, 1198.2, 1162.8, 1080.7 cm⁻¹; ¹H NMR (500 MHz, DMSO-*d*₆) δ 8.85 (t, *J* = 5.6 Hz, 1H), 8.18 (d, *J* = 9.0 Hz, 1H), 8.09 (s, 1H), 7.83 (t, *J* = 7.9 Hz, 1H), 7.77–7.68 (m, 3H), 7.45–7.34 (m, 2H), 5.53 (s, 1H), 3.30–3.26 (m, 4H), 3.03–3.01 (m, 2H), 2.92–2.85 (m, 2H), 1.82–1.77 (m, 2H), 1.67–1.55 (m, 8H). ¹³C NMR (125 MHz, DMSO-*d*₆) δ 191.41, 181.00, 165.97, 163.76, 161.34, 161.12, 150.20, 146.54, 141.80, 137.47, 133.47, 133.27, 132.50, 126.60, 125.10, 124.43, 124.31, 122.96, 122.28, 120.33, 119.36, 117.49, 117.38, 116.01, 49.35, 36.39, 36.36, 31.22, 27.94, 27.70, 26.97, 26.32; ESI-MS *m/z*: 548.2 [M – H]⁻; HRMS: calcd for C₃₃H₃₀N₃O₅ [M – H]⁻, 548.2191, found 548.2189.

4,5-Dihydroxy-9,10-dioxo-N-(4-((7,8,9,10-tetrahydro-6H-cyclohepta[b]quinolin-11-yl)amino)butyl)-9,10-dihydroanthracene-2-carboxamide (**10l**). Intermediate **9** was treated with **8m** according to the general procedure to give the desired product **10l** as a red solid in 60.0% yield, m.p. 152–154 °C; IR (KBr) ν 3444.9, 2922.8, 1633.2, 1566.1, 1472.8, 1453.1, 1400.8, 1270.9, 1199.3, 1080.1 cm⁻¹; ¹H NMR (500 MHz, DMSO-*d*₆) δ 8.86 (t, *J* = 5.6 Hz, 1H), 8.16 (dd, *J* = 8.4, 1.3 Hz, 1H), 8.10 (d, *J* = 1.7 Hz, 1H), 7.82 (t, *J* = 7.9 Hz, 1H), 7.75–7.72 (m, 3H), 7.56–7.53 (m, 1H), 7.42–7.39 (m, 2H), 5.42 (t, *J* = 6.9 Hz, 1H), 3.33–3.24 (m, 4H), 3.10–3.00 (m, 2H), 2.96–2.87 (m, 2H), 1.80 (q, *J* = 6.0 Hz, 2H), 1.71–1.56 (m, 8H). ¹³C NMR (125 MHz, DMSO-*d*₆) δ 191.32, 181.06, 164.38, 163.81, 161.41, 161.25, 150.09, 145.76, 141.78, 137.40, 133.50, 133.29, 127.98, 127.93, 124.46, 124.10, 122.76, 122.71, 122.38, 121.75, 119.29, 117.41, 116.05, 49.44, 36.36, 31.31, 30.35, 27.97, 27.87, 27.05, 26.47, 26.38; ESI-MS *m/z*: 578.3 [M + H]⁺; HRMS: calcd for C₃₅H₃₆N₃O₅ [M + H]⁺, 578.2649, found 578.2651.

4,5-Dihydroxy-9,10-dioxo-N-(6-((7,8,9,10-tetrahydro-6H-cyclohepta[b]quinolin-11-yl)amino)hexyl)-9,10-dihydroanthracene-2-carboxamide (**10m**). Intermediate **9** was treated with **8l** according to the general procedure to give the desired product **10m** as a red solid 52.8% yield, m.p. 146–148 °C; IR (KBr) ν 3456.9, 2925.6, 1629.3, 1566.1, 1477.0, 1453.7, 1403.0, 1271.1, 1209.5, 1085.0 cm⁻¹; ¹H NMR (500 MHz, DMSO-*d*₆) δ 8.82 (t, *J* = 5.6 Hz, 1H), 8.14 (d, *J* = 8.4 Hz, 1H), 8.09–8.08 (m, 1H), 7.82–7.78 (m, 1H), 7.76–7.68 (m, 3H), 7.53 (t, *J* = 7.5 Hz, 1H), 7.43–7.34 (m, 2H), 5.31 (t, *J* = 6.6 Hz, 1H), 3.31–3.24 (m, 2H), 3.22 (q, *J* = 7.5, 6.8 Hz, 2H), 3.08–2.98 (m, 2H), 2.93–2.85 (m, 2H), 1.83–1.78 (m, 2H), 1.68–1.59 (m, 4H), 1.59–1.56 (m, 2H), 1.56–1.50 (m, 2H), 1.37–1.27 (m, 4H). ¹³C NMR (125 MHz, DMSO-*d*₆) δ 191.25, 181.04, 164.49, 163.78, 161.44, 161.33, 150.07, 145.93, 141.82, 137.35, 133.48, 133.27, 128.14, 127.82, 124.46, 124.02, 122.74, 122.69, 122.42, 121.81, 119.25, 117.37, 116.03, 49.64, 31.30, 30.37, 28.68, 27.92, 27.06, 26.50, 26.18, 26.09; ESI-MS *m/z*: 584.2 [M + H]⁺; HRMS: calcd for C₃₃H₃₁ClN₃O₅ [M + H]⁺, 584.1947, found 584.1950.

N-(6-((3-Chloro-7,8,9,10-tetrahydro-6H-cyclohepta[b]quinolin-11-yl)amino)hexyl)-4,5-dihydroxy-9,10-dioxo-9,10-dihydroanthracene-2-carboxamide (**10n**). Intermediate **9** was treated with **8n** according to the general procedure to give the desired product **10n** as a red solid in 51.5% yield, m.p. 139–141 °C; IR (KBr)

ν 3454.9, 2924.5, 1630.5, 1559.1, 1472.9, 1452.6, 1400.8, 1268.5, 1200.0, 1111.0 cm^{-1} ; ^1H NMR (500 MHz, CDCl_3) δ 8.05–7.98 (m, 1H), 7.91–7.88 (m, 1H), 7.86–7.79 (m, 2H), 7.76–7.66 (m, 2H), 7.36–7.29 (m, 2H), 6.45 (s, 1H), 3.49 (q, J = 6.7 Hz, 2H), 3.27 (t, J = 7.1 Hz, 2H), 3.17–3.10 (m, 2H), 2.91–2.82 (m, 2H), 1.90–1.85 (m, 2H), 1.79–1.75 (m, 2H), 1.73–1.69 (m, 2H), 1.69–1.64 (m, 4H), 1.50–1.42 (m, 4H). ^{13}C NMR (125 MHz, CDCl_3) δ 192.72, 181.25, 166.54, 165.10, 162.97, 162.88, 149.95, 142.72, 137.75, 135.97, 134.11, 133.57, 128.08, 125.58, 125.18, 123.82, 123.53, 122.46, 120.62, 120.49, 117.46, 117.18, 115.94, 50.71, 40.37, 32.02, 31.47, 29.84, 29.58, 28.31, 27.67, 26.90, 26.84, 26.78; ESI-MS m/z : 612.2 $[\text{M} + \text{H}]^+$; HRMS: calcd for $\text{C}_{35}\text{H}_{35}\text{ClN}_3\text{O}_5$ $[\text{M} + \text{H}]^+$, 612.2260, found 612.2262.

4.2. *In vitro* inhibition studies on AChE and BuChE

Acetylcholinesterase (AChE, E.C. 3.1.1.7, from the electric eel), butyrylcholinesterase (BuChE, E.C. 3.1.1.8, from equine serum), 5,5'-dithiobis-(2-nitrobenzoic acid) (Ellman's reagent, DTNB), S-butyrylthiocholine iodide (BTCI), acetylthiocholine iodide (ATCI), and tacrine hydrochloride were purchased from Sigma-Aldrich. The capacity of the test compounds (**1** and **10a–n**) to inhibit AChE and BuChE activities was assessed by Ellman's method.³⁸ A stock solution of test compounds was dissolved in a minimum volume of DMSO (1%) and was diluted using the buffer solution (50 mM Tris-HCl, pH = 8.0, 0.1 M NaCl, 0.02 M $\text{MgCl}_2 \cdot 6\text{H}_2\text{O}$). In 96-well plates, 160 μL of 1.5 mM DTNB, 50 μL of AChE (0.22 U mL^{-1} prepared in 50 mM Tris-HCl, pH = 8.0, 0.1% w/v bovine serum albumin, BSA) or 50 μL of BuChE (0.12 U mL^{-1} prepared in 50 mM Tris-HCl, pH = 8.0, 0.1% w/v BSA) were incubated with 10 μL of various concentrations of test compounds (0.001–100 μM) at 37 °C for 6 min followed by the addition of the substrates (30 μL) acetylthiocholine iodide (15 mM) or S-butyrylthiocholine iodide (15 mM) and the absorbance was measured at different time intervals (0, 60, 120, and 180 s) at a wavelength of 405 nm. The concentration of the compound producing 50% of enzyme activity inhibition (IC_{50}) was calculated by non-linear regression analysis of the response–concentration (log) curve, using the Graph-Pad Prism program package (GraphPad Software; San Diego, CA). Results are expressed as the mean \pm SEM of at least three different experiments performed in triplicate.

4.3. Kinetic analysis of ChE inhibition

To obtain the mechanism of action of **10b**, reciprocal plots of $1/\text{velocity}$ versus $1/[\text{substrate}]$ were constructed at different concentrations of the substrate thiocholine iodide (0.05–0.5 mM) by using Ellman's method. Three concentrations of **10b** were selected for the studies: 13.6, 27.3 and 54.6 nM for the kinetic analysis of AChE inhibition, and 100, 200, 400 nM for the kinetic analysis of BuChE inhibition, respectively. The plots were assessed by a weighted least-squares analysis that assumed the variance of velocity (ν) to be a constant percentage of ν for the entire data set. Slopes of these reciprocal plots were then plotted against the concentration of **10b** in a

weighted analysis and K_i was determined as the intercept on the negative x -axis. Data analysis was performed with Graph-Pad Prism 4.03 software (GraphPad Software Inc.).

4.4. Molecular modeling studies

Molecular modeling calculations and docking studies were performed using Molecular Operating Environment (MOE) software version 2008.10 (Chemical Computing Group, Montreal, Canada). The X-ray crystallographic structure of AChE complexed with bis(7)-tacrine (PDB code 2CKM) was obtained from the Protein Data Bank. All water molecules in PDB files were removed and hydrogen atoms were subsequently added to the protein. The compound **10b** was built using the builder interface of the MOE program and the energy minimized using the MMFF94x force field. Then the **10b** was docked into the active site of the protein by the "Triangle Matcher" method, which generated poses by aligning the ligand triplet of atoms with the triplet of alpha spheres in cavities of tight atomic packing. The Dock scoring in MOE software was done using the ASE scoring function and Forcefield was selected as the refinement method. The best 10 poses of molecules were retained and scored. After docking, the geometry of the resulting complex was studied using MOE's pose viewer utility.

4.5. Inhibition of AChE-induced A β (1–40) aggregation

Inhibition of AChE-induced A β aggregation was measured using a Thioflavin T (ThT)-binding assay.^{41,42} Aliquots of 2 μL of A β (1–40) (Anaspec Inc.), lyophilized from 2 mg mL^{-1} HFIP (1,1,1,3,3,3-hexafluoro-2-propanol) and dissolved in DMSO, were incubated for 24 h at room temperature in 0.215 M sodium phosphate buffer (pH 8.0) at a final concentration of 230 μM . For co-incubation experiments, aliquots of AChE (16 μL , 0.6 U mL^{-1} , final concentration) and AChE in the presence of the tested compound (2 μL , 100 μM , final concentration) were added. Blanks containing A β , AChE, A β plus the tested compound in 0.215 M sodium phosphate buffer (pH 8.0) were prepared. After incubation, the samples were diluted to a final volume of 200 μL with 50 mM glycine–NaOH buffer (pH 8.0) containing thioflavin T (1.5 μM). Then the fluorescence intensities were measured on a SpectraMax M5 (Molecular Devices, Sunnyvale, CA, USA) multi-mode plate reader with excitation and emission wavelengths at 446 nm and 490 nm, respectively. Each inhibitor was examined in triplicate. The percent inhibition of the AChE-induced aggregation due to the presence of the inhibitor was calculated by the following formula: $100 - (\text{IF}_i/\text{IF}_o \times 100)$, where IF_i and IF_o are the fluorescence intensities obtained for A β plus AChE in the presence and in the absence of the inhibitor, respectively, minus the fluorescent intensities due to the respective blanks.

4.6. Spectrophotometric measurement of the complex with Cu^{2+} and Fe^{2+}

The study of metal chelation was performed in methanol at 298 K using a UV-vis spectrophotometer (SHIMADZU UV-2450PC) with wavelength ranging from 200 to 500 nm.⁴⁴ The difference UV-vis spectra due to complex formation were

obtained by numerical subtraction of the spectra of the metal alone and the compound alone (at the same concentration used in the mixture) from the spectra of the mixture. A fixed amount of **10b** ($25 \mu\text{mol L}^{-1}$) was mixed with growing amounts of copper ions ($2\text{--}50 \mu\text{mol L}^{-1}$) and the difference UV-vis spectra were tested to investigate the ratio of the ligand/metal in the complex.

The stoichiometry of the complex **10b**- Cu^{2+} was measured by using Job's method.⁴⁵ From separation of hybrid **10b** and CuCl_2 in Tris buffer, both of the same concentration ($25 \mu\text{mol L}^{-1}$), 17 solutions were obtained under the condition that the sum of concentrations of both species was a constant in all samples but the proportions of both components varied between 0 and 100%. The absorbance differences at 250 nm were plotted vs. the mole fraction, showing a maximum at 0.53 that revealed a stoichiometry of 1 : 1 for complex **10b**- Cu^{2+} .

4.7. Hepatotoxicity studies

The experiments were carried out on adult male ICR mice (weighing 18–22 g), which were purchased from the Comparative Medicine Centre, Yangzhou University. Tacrine hydrochloride hydrate was dissolved in CMC-Na solution (0.5 g CMC-Na in 100 mL of distilled water) and 3 mg per 100 g b wt, corresponding to $11.86 \mu\text{mol}$ per 100 g b wt, were administered id. Test compounds were dissolved in CMC-Na solution, and an equimolar dose corresponding to tacrine was administered id. Heparinized serum was obtained 8, 20, and 30 h after dosing from the retrobulbar plexus to determine aspartate aminotransferase (ASAT) and alanine aminotransferase (ALT) activity, two indicators of a liver damage, using routine methods.

For morphological studies, tacrine and tested compound treated rats were sacrificed in ether anesthesia 30 h after dosing, and livers were harvested. Two 3 mm sections of each liver extending from the hilus to the margin of the left lateral lobe were immediately placed in 10% buffered formaldehyde, fixed for two days, and embedded together in one paraffin block. Subsequently, $5 \mu\text{m}$ sections were prepared from these paraffin blocks. Paraffin sections of each block were deparaffinated and stained with hematoxylin and eosin or by means of the periodic acid-Schiff procedure for glycogen.

Acknowledgements

This research work was financially supported by the Innovative Research Team in University (IRT1193), a project funded by the Priority Academic Program Development of Jiangsu Higher Education Institutions (PAPD), Project of Graduate Education Innovation of Jiangsu Province (no. CXZZ13_0320).

Notes and references

- V. H. Finder, *J. Alzheimers Dis.*, 2010, **22**(Suppl 3), 5.
- E. D. Roberson and L. Mucke, *Science*, 2006, **314**, 781.
- C. X. Gong and K. Iqbal, *Curr. Med. Chem.*, 2008, **15**, 2321.
- R. T. Bartus, R. L. Dean 3rd, B. Beer and A. S. Lippa, *Science*, 1982, **217**, 408.
- D. Pratico, *Ann. N. Y. Acad. Sci.*, 2008, **1147**, 70.
- G. Pepeu and M. G. Giovannini, *Curr. Alzheimer Res.*, 2009, **6**, 86.
- M. Villarroya, A. G. Garcia, J. Marco-Contelles and M. G. Lopez, *Expert Opin. Invest. Drugs*, 2007, **16**, 1987.
- M. Esquivias-Perez, E. Maalej, A. Romero, F. Chabchoub, A. Samadi, J. Marco-Contelles and M. J. Oset-Gasque, *Chem. Res. Toxicol.*, 2013, **26**, 986.
- Y. Chen, J. Sun, L. Fang, M. Liu, S. Peng, H. Liao, J. Lehmann and Y. Zhang, *J. Med. Chem.*, 2012, **55**, 4309.
- M. Harel, L. K. Sonoda, I. Silman, J. L. Sussman and T. L. Rosenberry, *J. Am. Chem. Soc.*, 2008, **130**, 7856.
- Y. Bourne, P. Taylor, Z. Radic and P. Marchot, *EMBO J.*, 2003, **22**, 1.
- A. E. Reyes, M. A. Chacon, M. C. Dinamarca, W. Cerpa, C. Morgan and N. C. Inestrosa, *Am. J. Pathol.*, 2004, **164**, 2163.
- A. Castro and A. Martinez, *Curr. Pharm. Des.*, 2006, **12**, 4377.
- E. Giacobini, *Pharmacol. Res.*, 2004, **50**, 433.
- J. Hardy and D. J. Selkoe, *Science*, 2002, **297**, 353.
- C. Supnet and I. Bezprozvanny, *J. Alzheimers Dis.*, 2010, **20**(Suppl 2), S487.
- F. Belluti, M. Bartolini, G. Bottegoni, A. Bisi, A. Cavalli, V. Andrisano and A. Rampa, *Eur. J. Med. Chem.*, 2011, **46**, 1682.
- A. I. Bush, *J. Alzheimers Dis.*, 2008, **15**, 223.
- D. G. Smith, R. Cappai and K. J. Brnham, *Biochim. Biophys. Acta*, 2007, **1768**, 1976.
- X. Huang, R. D. Moir, R. E. Tanzi, A. I. Bush and J. T. Rogers, *Ann. N. Y. Acad. Sci.*, 2004, **1012**, 153.
- X. Huang, C. S. Atwood, M. A. Hartshorn, G. Multhaup, L. E. Goldstein, R. C. Scarpa, M. P. Cuajungco, D. N. Gray, J. Lim, R. D. Moir, R. E. Tanzi and A. I. Bush, *Biochemistry*, 1999, **38**, 7609.
- P. B. Watkins, H. J. Zimmerman, M. J. Knapp, S. I. Gracon and K. W. Lewis, *JAMA*, 1994, **271**, 992.
- A. Musial, M. Bajda and B. Malawska, *Curr. Med. Chem.*, 2007, **14**, 2654.
- V. Tumiatti, A. Minarini, M. L. Bolognesi, A. Milelli, M. Rosini and C. Melchiorre, *Curr. Med. Chem.*, 2010, **17**, 1825.
- M. I. Rodriguez-Franco, M. I. Fernandez-Bachiller, C. Perez, B. Hernandez-Ledesma and B. Bartolome, *J. Med. Chem.*, 2006, **49**, 459.
- M. I. Fernandez-Bachiller, C. Perez, L. Monjas, J. Rademann and M. I. Rodriguez-Franco, *J. Med. Chem.*, 2012, **55**, 1303.
- L. Fang, D. Appenroth, M. Decker, M. Kiehntopf, C. Roegler, T. Deufel, C. Fleck, S. Peng, Y. Zhang and J. Lehmann, *J. Med. Chem.*, 2008, **51**, 713.
- J. Cyong, T. Matsumoto, K. Arakawa, H. Kiyohara, H. Yamada and Y. Otsuka, *J. Ethnopharmacol.*, 1987, **19**, 279.

- 29 M. L. Lin, J. G. Chung, Y. C. Lu, C. Y. Yang and S. S. Chen, *Oral Oncol.*, 2009, **45**, 531.
- 30 Y. L. Zhao, G. D. Zhou, H. B. Yang, J. B. Wang, L. M. Shan, R. S. Li and X. H. Xiao, *Food Chem. Toxicol.*, 2011, **49**, 1705.
- 31 M. Z. Guo, X. S. Li, H. R. Xu, Z. C. Mei, W. Shen and X. F. Ye, *Acta Pharmacol. Sin.*, 2002, **23**, 739.
- 32 X. Wang, H. Sun, A. Zhang, G. Jiao, W. Sun and Y. Yuan, *Analyst*, 2011, **136**, 5068.
- 33 A. Zhang, H. Sun and X. Wang, *Eur. J. Med. Chem.*, 2013, **63**, 570.
- 34 J. Liu, G. Hu, R. Xu, Y. Qiao, H. P. Wu, X. Ding, P. Duan, P. Tu and Y. J. Lin, *J. Asian Nat. Prod. Res.*, 2013, **15**, 756.
- 35 S. Y. Li, X. B. Wang, S. S. Xie, N. Jiang, K. D. Wang, H. Q. Yao, H. B. Sun and L. Y. Kong, *Eur. J. Med. Chem.*, 2013, **69**, 632.
- 36 Y. F. Han, C. P. Li, E. Chow, H. Wang, Y. P. Pang and P. R. Carlier, *Bioorg. Med. Chem.*, 1999, **7**, 2569.
- 37 J. Cai, Y. Duan, J. Yu, J. Chen, M. Chao and M. Ji, *Eur. J. Med. Chem.*, 2012, **55**, 409.
- 38 G. L. Ellman, K. D. Courtney, V. Andres Jr. and R. M. Feather-Stone, *Biochem. Pharmacol.*, 1961, **7**, 88.
- 39 M. Recanatini, A. Cavalli, F. Belluti, L. Piazzzi, A. Rampa, A. Bisi, S. Gobbi, P. Valenti, V. Andrisano, M. Bartolini and V. Cavrini, *J. Med. Chem.*, 2000, **43**, 2007.
- 40 M. K. Hu, L. J. Wu, G. Hsiao and M. H. Yen, *J. Med. Chem.*, 2002, **45**, 2277.
- 41 H. Tang, L. Z. Zhao, H. T. Zhao, S. L. Huang, S. M. Zhong, J. K. Qin, Z. F. Chen, Z. S. Huang and H. Liang, *Eur. J. Med. Chem.*, 2011, **46**, 4970.
- 42 M. Bartolini, C. Bertucci, V. Cavrini and V. Andrisano, *Biochem. Pharmacol.*, 2003, **65**, 407.
- 43 P. Camps, X. Formosa, C. Galdeano, T. Gomez, D. Munoz-Torrero, M. Scarpellini, E. Viayna, A. Badia, M. V. Clos, A. Camins, M. Pallas, M. Bartolini, F. Mancini, V. Andrisano, J. Estelrich, M. Lizondo, A. Bidon-Chanal and F. J. Luque, *J. Med. Chem.*, 2008, **51**, 3588.
- 44 R. Joseph, B. Ramanujam, A. Acharya, A. Khutia and C. P. Rao, *J. Org. Chem.*, 2008, **73**, 5745.
- 45 M. I. Fernandez-Bachiller, C. Perez, G. C. Gonzalez-Munoz, S. Conde, M. G. Lopez, M. Villarroya, A. G. Garcia and M. I. Rodriguez-Franco, *J. Med. Chem.*, 2010, **53**, 4927.
- 46 J. P. Mackeigan, K. R. Martin, S. Gately and T. Wang, *Int. Pat.*, WO 2012154879, 2012.
- 47 J. J. Bornstein, T. J. Eckroat, J. L. Houghton, C. K. Jones, K. D. Green and S. Garneau-Tsodikova, *Med. Chem. Commun.*, 2011, **2**, 406.
- 48 C. M. Lee, *J. Med. Chem.*, 1968, **11**, 388.
- 49 P. Szymanski, M. Markowicz, M. Bajda, B. Malawska and E. Mikiciuk-Olasik, *Lett. Drug Des. Discovery*, 2012, **9**, 645.